Korean J. Chem. Eng., 15(1), 28-36 (1998)

SIMULATION OF PERVAPORATION PROCESS FOR ETHANOL DEHYDRATION BY USING PILOT TEST RESULTS

Jae-Hwa Chang†, Je-Kang Yoo, Seung-Ho Ahn, Kyu-Hyun Lee and Suk-Moon Ko*

R&D Center, Sunkyong Engineering & Construction Ltd., 192-18, Kwanhun-dong, Chongro-gu, Seoul, Korea
*Department of Environmental Engineering, College of Engineering, University of Ulsan, Ulsan 680-749, Korea
(Received 21 June 1997 • accepted 14 October 1997)

Abstract – This paper focuses on providing a pervaporation simulation method for ethanol dehydration from a practical point of view. The simulation procedure is performed by setting up simulation equations which describe the pervaporation process, obtaining the necessary data from pervaporation batch mode pilot tests, verifying the simulation tool through simulations of continuous mode pilot tests, and comparing the simulation results with the real pilot test results. We considered the mass and energy balances that describe separating an ethanol/water mixture by a pervaporation membrane. The simulation equations were mathematically expressed into simultaneous nonlinear differential equations based on these balances. The necessary data for simulation consist of the thermophysical properties for the ethanol-water mixture and the characteristic data of a PVA composite membrane. The membrane characteristic data are permeation flux and membrane selectivity, which are functions of feed composition and operating conditions. These data were experimentally determined by a batch mode pilot test. The continuous mode pilot tests were simulated and the simulation results were compared to the real test results. The results were fairly good.

Key words: Pervaporation, Simulation, Ethanol Dehydration, Pilot Test, Membrane Characteristic Data

INTRODUCTION

Ethanol is currently produced by fermentation or from the hydration of ethylene. Fermented ethanol is used mainly in the food industry, while synthetic ethanol is used in solvent and chemical applications. In the United States and Brazil, fermentation processes have become the primary source of ethanol since production of ethanol by fermentation processes grew in response to rising crude oil prices during the mid-1970s. The bulk of fermentation ethanol is used primarily as an additive, about 10 %, to extend gasoline for automotive fuels in both of these countries. The ethanol-blended gasoline is marketed under the fuel name, gasohol. Not only is it naturally renewable, but gasohol has lower emissions of carbon monoxide, carbon dioxide and hydrocarbon. The consumption of petroleum-based fuels could also be reduced if the gasohol was used as a motor fuel. The purity of ethanol used for fuel additives is usually anhydrous ethanol of above 99 % [Black, 1980]. In Korea, most anhydrous ethanol is consumed in solvent applications and as a chemical raw material. Considering environmental and energy issues, a rapid growth in demand is expected in the near future for anhydrous ethanol as a motor fuel. It is expected that the demand for ethanol as a raw material to produce ethyl *tert*-butyl ether (ETBE) will increase. ETBE is an environmentally friendly alternative compared to methyl *tert*-butyl ether (MTBE) which, at the present, is largely used as an octane enhancer added to gasoline [Streicher et al., 1995].

Regardless of the source of the ethanol, from fermentation or from direct hydration of ethylene, the product is normally a dilute aqueous solution. The product is fed to a distillation system to concentrate ethanol. The separation of ethanol and water is complicated by the fact that ethanol and water form an azeotrope at 95.6 weight % ethanol. It is impossible to produce pure ethanol from an azeotropic mixture by normal distillation: at the azeotropic composition the composition of the vapor coming off is the same as that of the liquid. For dehydration of ethanol, there are several methods. One such conventional process involved is azeotropic distillation in which the entrainer is added to break the azeotrope [Black, 1980]. Benzene, cyclohexane and N-pentane etc. can be used as entrainer. In azeotropic distillation, the entrainer lowers the boiling point of the ethanol-water mixture and ties up the water. The entrainer-ethanol-water mixture is removed as vapor from the top of the distillation column, while pure ethanol remains as liquid at the bottom of the column. The entrainer in this case must be completely removed and recovered from both product streams. The energy input may be considerable compared to other processes such as adsorption and pervaporation. In adsorption, the water is removed by adsorption agents (molecular sieve) which adsorb more polar water molecules than ethanol molecules by weak molecular forces, while the ethanol molecules simply pass over the sieves [Humphrey and Seibert, 1992]. However, the amount of adsorption agents increases strongly with increasing amount of water to be removed and with decreasing final concentration of water in the product. In addition, it is usually difficult to regenerate

†To whom all correspondence should be addressed.
E-mail: jhchang@cosmos.skec.co.kr

the adsorption agent; moreover, the recovery yield of ethanol is lower than the other processes. Pervaporation is a method for dehydration of organics such as ethanol, which substantially avoids the above-mentioned drawbacks of azeotropic distillation and adsorption [Fleming, 1992]. As the pervaporation membrane process is not governed by thermodynamic equilibria and selectivity is determined by the difference in permeation rates of components through the membrane, mixtures of components with close boiling points and azeotropic mixtures can be effectively separated [Aptel et al., 1976; Rautenbach and Albrecht, 1985a, b]. According to this method, the mixture to be dehydrated is contacted with the feed side of a non-porous membrane, where this membrane has a particularly high permeability to water, while ethanol passes only to a very small degree. Compared to conventional membrane processes such as ultrafiltration or reverse osmosis, fluxes in pervaporation are generally low (<10 kg/m^2-h). However, selectivities can be extremely high, often exceeding 1,000. Transport of the permeate through the non-porous pervaporation membrane can be generally described as a series of three events: preferential sorption of mixture components, diffusion across the membrane and desorption on the permeate side [Binning et al., 1961; Mulder and Smolders, 1984; Mulder et al., 1985]. However, it is not entirely clear what is going on in the pervaporation membrane.

Driven by the need for environmentally friendly energy-saving process technology, research on pervaporation took off in the 1980s and the first commercial systems hit the market. Today, about 100 commercial plants have been installed, from pilot plants with 1-to 4 m^2 membranes to fuel-ethanol dehydration units with 2,100 m^2 membranes processing up to 5,000 kg/h [Rapin, 1988]. Half of the commercial plants are in operation for dehydration of ethanol. The development of an asymmetric composite membrane, manufactured by Deutsche Carbone in Germany, made it possible to commercialize the pervaporation system [Tusel and Bruschke, 1985]. The membranes for water permeation utilize a supporting layer such as a nonwoven porous polyester on which is cast either a polyacrylonitrile (PAN) or polysulfone (PS) ultrafiltration membrane, and finally a 0.1-μm thick layer of cross-linked polyvinyl alcohol(PVA) which provides separation. Pervaporation exhibits its highest efficiency in a concentration range of the ethanol-water mixture where distillation is least effective, namely, at high ethanol concentration, especially in the vicinity of azeotropic concentration. For this reason, most pervaporation plants for ethanol dehydration have been retrofitted to existing distillation trains in order to increase plant capacity, as well as to produce higher purity product ethanol.

For a pervaporation system to be simulated accurately, a reasonable method for estimating the parameters for membrane characteristics is needed, because membrane characteristic data such as permeability and selectivity are influenced by feed composition and operating conditions [Marin et al., 1992]. Also, the results of pervaporation tests may be dependent on the size of membrane module used. Scaling-up by extrapolating the results acquired from membranes with small surface areas, for instance, in cell tests may, therefore, in certain cases, lead to unpleasant surprises. The main reason is that the feed flow pattern at the feed side can be changed as the membrane area is increased, which results in unsatisfactory hydrodynamics in the membrane module used in scaling-up the pervaporation system. Therefore, the purpose of this paper is to present a method of pervaporation simulation for accurate prediction of a practical pervaporation process for ethanol dehydration. This paper begins by describing the simulation equations based on mass and energy balances, and provides an estimation method of parameters that are necessary for simulation. Then the suitability of simulation is verified by comparing the simulation results with the experimental data. The parameters for the simulation of ethanol dehydration by pervaporation are obtained from a batch mode pilot test that has a moderately large membrane. The membrane used is a PVA composite membrane that is commercially used for ethanol dehydration. Continuous mode pilot tests, which can be operated in the same manner as in full-scale plants, are conducted to verify the suitability of the simulation tool.

SIMULATION EQUATIONS

A schematic flow diagram of the pervaporation process is presented in Fig. 1. The feed mixture, usually in the liquid phase, is heated by passing through a preheater and a heater. The feed flows through the pervaporation membrane module, where it passes along the membranes. The membrane separates a mixture into two compartments: the feed (retentate) and permeate compartments. The permeate to be removed is vaporized through the membranes and then condensed and purged out. The driving force for permeation through the membrane is the difference in partial pressure of the permeating substances. The partial pressure on the permeate side is lowered by having a vacuum pump and a cooling system to condense the permeate vapor. In this case, the vacuum pump is only used for the removal of non-condensables. The pervaporation process is perpetually driven by condensation of the permeate, creating a significant vacuum and requiring lower temperatures on the permeate side of the membrane. It is also important to keep the temperature of the feed as high as is practical: as the temperature falls, so will the permeation flux across the membrane. The vaporization through the membrane cools down the processed feed fluid, which must be reheated to maintain the highest flux through membranes.

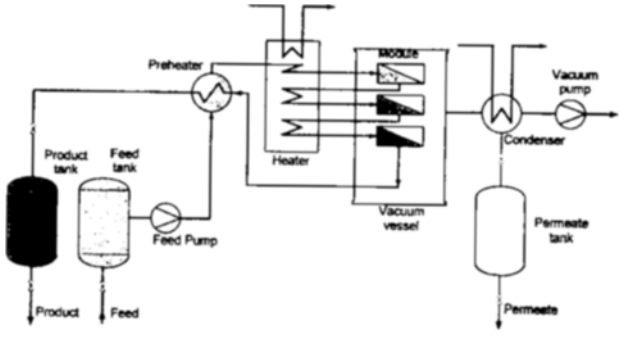

Fig. 1. Schematic flow diagram of pervaporation process.

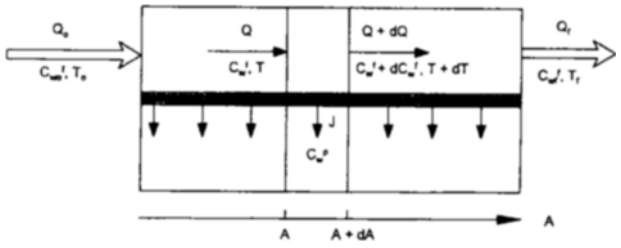

Fig. 2. Differential element of pervaporation membrane module as used in the simulation of the pervaporation system.

For this reason, the membrane module is divided into several stages with interstage heaters.

In the following, we will present a pervaporation simulation equation which is valid for the dehydration of ethanol [Chang et al., 1997]. Fig. 2 shows a simplified picture of a pervaporation membrane module for the separation of a binary ethanol-water mixture. As shown in Fig. 2, pervaporation resembles a continuous flow process, which makes it possible to concentrate ethanol by extracting a permeate enriched in water. The assumptions in this model are (1) Plug-flow along the feed side of the membrane, (2) Cross-flow along the permeate side of the membrane, (3) No polarization effect or permeate pressure losses, (4) Unhindered permeate flux, and (5) Constant permeate composition in the membrane module and vessel.

The following differential equations are used to describe the separation of water and ethanol by a hydrophilic pervaporation membrane, and these formulate the mass and energy balances for the elementary volume in Fig. 2. The change in the feed flow rate along the feed side of the membrane is expressed by the total permeation flux, J_t.

$$\frac{dQ}{dA} = -J_t \tag{1}$$

where Q is the feed flow rate, and dA is an element of membrane area.

The change in composition along the feed side of the membrane can be obtained from a mass balance with respect to the more permeable water component.

$$\frac{dC_w^f}{dA} = \frac{J_t(C_w^f - C_w^p)}{Q} \tag{2}$$

In Eq. (2), C_w^f and C_w^p are the water concentrations in the feed and permeate side, respectively. The major part of the energy consumed in pervaporation corresponds to the heat required to vaporize the permeate, which is supplied by liquid feed. As a result, the temperature of the flowing feed decreases as it proceeds along the membrane. Pervaporation is far from being an isothermal process in which a definite temperature profile is established between the entrance and exit of each stage of the membrane module.

$$\frac{dT}{dA} = -\frac{J_t \cdot \Delta H}{Q \cdot k} \tag{3}$$

where T is the temperature in the feed side, ΔH is the latent heat of vaporization of permeate, and k is the liquid heat capacity of feed. Boundary conditions in these differential equations are given at the entrance:

$$\begin{aligned} &Q = Q_o && \text{at } A = 0 \\ &C_w^f = C_{wo}^f && \text{at } A = 0 \\ &T = T_o && \text{at } A = 0 \end{aligned} \tag{4}$$

ΔH and k are deduced through linear interpolation, from the values of the individual pure components.

$$\Delta H = C_w^p \cdot \Delta H_w + (1 - C_w^p) \cdot \Delta H_e \tag{5}$$

$$k = C_w^f \cdot k_w + (1 - C_w^f) \cdot k_e \tag{6}$$

These equations are coupled and integrated by a numerical method such as the Runge-Kutta algorithm. For this calculation, the total permeation flux and permeate composition have to be given as functions of the feed concentration and operating conditions such as temperature in the feed side and permeate pressure.

EXPERIMENTAL

1. Material & Apparatus

The ethanol dehydration tests were conducted on a pervaporation pilot unit that, except for the membrane module parts, was designed and manufactured by our group. Fig. 3 shows a schematic diagram of a pervaporation pilot unit that has automated data acquisition, on-line sampling and analysis, and unattended operation. The membrane used was a composite membrane that has PVA as an active layer, and the membrane system was composed of a plate and frame module. The membrane system, which was supplied by Deutsche Carbone GFT, consisted of two modules. Each module has two stages, the membrane area is 1 m^2 at each stage, and all stages are incorporated with an interstage heater. The feed ethanol was purchased from Korea Alcohol Industry, and the ethanol was produced by catalytic hydration of ethylene and concentrated to an ethanol-rich mixture.

2. Method

Pilot tests were conducted in two modes, batch and continuous, as shown in Fig. 4. To reach the high ethanol con-

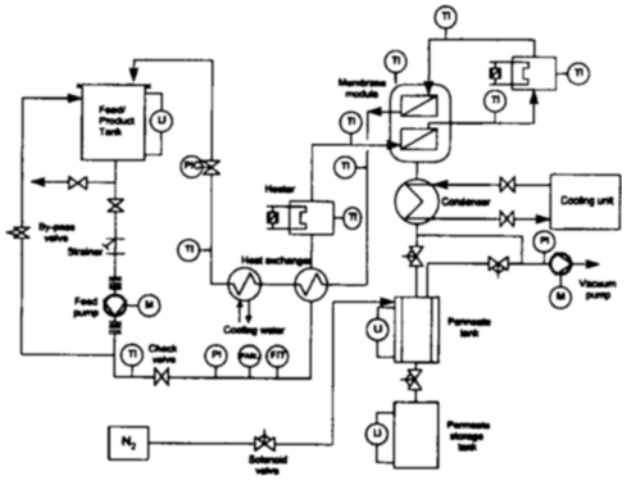

Fig. 3. Schematic diagram of pervaporation pilot unit.

centrations required, despite the small surface area of the membranes, the batch mode acts as a closed loop: after passing through the membrane modules, the retentate returns to the feed tank. In the continuous mode, we investigated the degree of ethanol dehydration performed by the pervaporation system, which has a membrane area of 4 m^2, in once-through mode operation.

In the batch mode, we measured the compositions of feed and permeate along with permeate amount as functions of operation time by varying the temperature on the feed side of the membrane and the permeate pressure, which is dependent on the permeate condensation temperature. Since we observed slight variations in the temperature on the feed side and the permeate condensation temperature and permeate pressure while running pilot tests, the average values were chosen as the values of these operating conditions. For the batch mode pilot test, the feed circulation flow rate was 80 *l*/hr, and the variation of temperature drop in the membrane stage was not large. In the continuous mode, the operation was carried out without returning the retentate to the feed tank so that the concentration of feed, product and permeate could be measured in a steady state. The flow rates in continuous mode pilot tests are lower than in batch mode pilot tests. The reason for operating at lower flow rates is that total membrane area of 4 m^2 is too small to dehydrate the larger amount of ethanol. The permeate flux was measured by weighing the permeate collected in a permeate tank. The ethanol concentrations in the feed and permeate (including product in the continuous mode) were measured on a Shimadzu GC-14B gas chromatograph with a column packed with Porapak-Q and thermal conductivity detector (TCD). Table 1 shows the operating conditions of the batch and continuous mode pilot test.

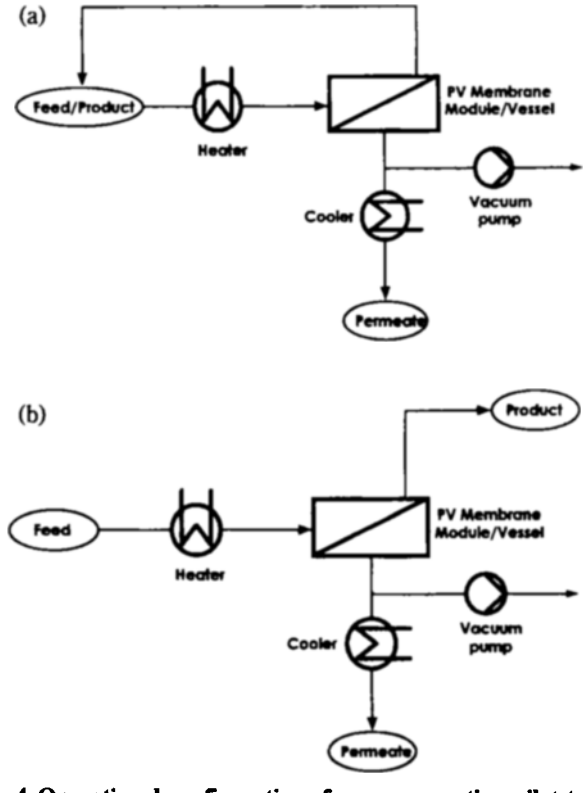

Fig. 4. Operational configurations for pervaporation pilot test.
(a) batch recycle mode, (b) continuous mode.

Table 1. Operating conditions of pervaporation pilot test

Batch mode
- Feed concentration: 91-93 wt% ethanol
- Average temperature in the feed side of the membrane module: 70, 78, 86, 90 °C
- Permeate condensation temperature: −10, 0, 18 °C
- Permeate pressure: 7, 11, 32 mbar
- Feed circulation flow rate: 80 *l*/h
- Operation time: 5 hrs

Continuous mode
- Feed concentration: 93.9, 98.8 wt% ethanol
- Feed temperature at module inlet: 95.3, 96.2 °C
- Permeate condensation temperature: −9, −10 °C
- Permeate pressure: 13 mbar
- Feed circulation flow rate: 15, 20 *l*/h

RESULTS AND DISCUSSION

1. Parameter Estimation from Batch Mode Pilot Test

As mentioned in describing the simulation equations, the necessary parameters for simulating a pervaporation system are the permeability and selectivity of the pervaporation membrane: the former is closely related to the permeation flux, and the latter is determined by the permeate composition. These membrane characteristic data are given as functions of feed composition and operating conditions such as feed side temperature and permeate pressure. However, it is difficult to determine these parameters theoretically, and they are not accurate enough to apply to simulation equations, although these can be obtained. Hence, in the practical design of the pervaporation process, these parameters are given as forms of empirical equations as functions of various variables. These empirical equations can provide results that are within the accuracy of the data available. We also determined the parameters from empirical equations that were obtained in the batch mode pilot tests. The simulation tool derived here is thus based on a black-box representation of the transport properties across the pervaporation membrane.

In batch mode tests, we periodically took samples of feed and permeate and analyzed their concentrations. From these data, we studied the selectivity dependence upon the feed composition, feed side temperature and permeate pressure. The results are shown in Fig. 5, which is a plot of permeate compositions versus feed concentration with varying operating conditions. As Fig. 5 indicates, the water content in the permeate is still high even with low water content in the feed. This implies high water selectivity of the pervaporation membrane that comes from the relative rates of transport of two components, water and ethanol, through the membrane. It is generally due to the preferential sorption and the difference in diffusive transport. Fig. 5 also shows that the membrane selectivity is found to be hardly altered by permeate pressure change when we separate the water/ethanol mixture in the vicinity of azeotropic composition with a PVA membrane, as

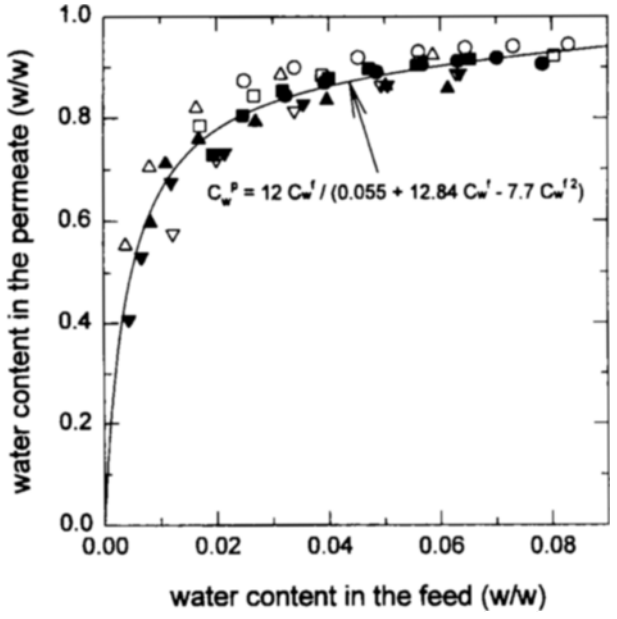

Fig. 5. Permeate concentration for the feed concentration with varying temperature in the feed side of the membrane and permeate pressure.
○, 70 °C, 11 mbar; □, 78 °C, 11 mbar; △, 86 °C, 11 mbar; ▽, 90 °C, 11 mbar; ●, 70 °C, 32 mbar; ■, 78 °C, 32 mbar; ▲, 78 °C, 7 mbar; ▼, 90 °C, 7 mbar.

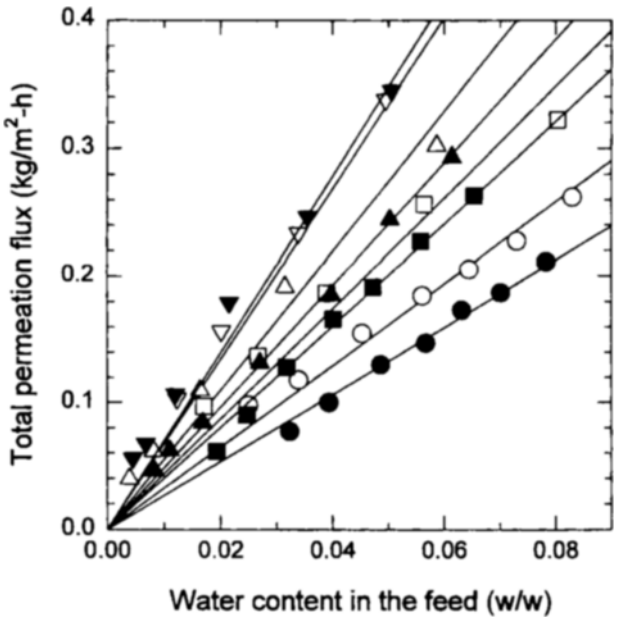

Fig. 6. Total permeation flux for the feed concentration with varying temperature in the feed side of the membrane and permeate pressure.
○, 70 °C, 11 mbar; □, 78 °C, 11 mbar; △, 86 °C, 11 mbar; ▽, 90 °C, 11 mbar; ●, 70 °C, 32 mbar; ■, 78 °C, 32 mbar; ▲, 78 °C, 7 mbar; ▼, 90 °C, 7 mbar.

long as the permeate pressure is sufficiently lower than the saturated vapor pressure of the permeate. The influence of temperature on the feed side on the selectivity can be neglected, which means that there is no difference in the increasing rate of fluxes with temperature between two components in a mixture.

We also periodically measured the amount of permeate with varying operating conditions. Fig. 6 shows the dependence of total permeation fluxes on the feed composition and operating conditions. The results shown in Fig. 6 demonstrate that the permeation fluxes increase linearly with the water content in the feed. The increase of permeation flux with the content of water, which interacts strongly with the membrane, can be interpreted as the dependence of diffusivity on concentration and higher extent of sorption of water. Since the driving force in pervaporation is obtained by the difference in partial pressure between feed and permeate, an increase in the vapor pressure in the permeate is equivalent to a decrease of the driving force for the transport. As a result, the permeation flux decreases with permeate pressure.

Fig. 7 shows the effect of feed composition on the partial water permeation fluxes. The partial permeation fluxes of water were determined by data on total fluxes and permeate compositions. This can be explained on the same basis with an interpretation for total permeation flux. The temperature dependence of permeation flux is also illustrated in Fig. 7. There is a strong dependence of flux on feed temperature because both sorption and diffusion govern the permeation through the pervaporation membrane. Since diffusion and sorption are the activated processes, the influence of temperature on the partial water permeation flux, J_w, can be described by an Arrhenius type law [Huang and Jarvis, 1970; Nguyen, 1986; Yeom et al., 1996].

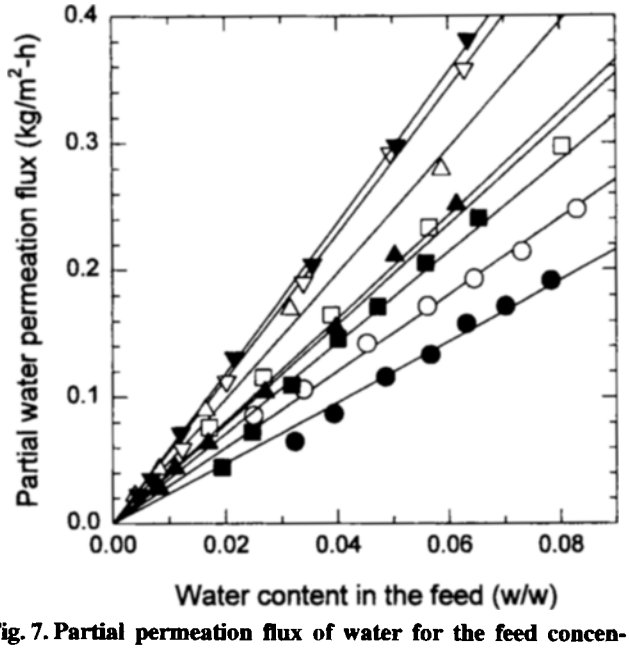

Fig. 7. Partial permeation flux of water for the feed concentration with varying temperature in the feed side of the membrane and permeate pressure.
○, 70 °C, 11 mbar; □, 78 °C, 11 mbar; △, 86 °C, 11 mbar; ▽, 90 °C, 11 mbar; ●, 70 °C, 32 mbar; ■, 78 °C, 32 mbar; ▲, 78 °C, 7 mbar; ▼, 90 °C, 7 mbar.

$$J_w = J_w^* \exp(-E_w/RT) \quad (7)$$

where J_w^* is the frequency factor, E_w is the activation energy for water permeation, and R is the gas constant. Experimental observation shows that the plot of the logarithm of partial water flux versus the reciprocal of absolute temperature generally falls on a straight line for a reasonably large temperature range from 70 to 90 °C (See Fig. 8). The slope in Fig. 8 is the Arrhenius coefficient, E_w/R, for which the value is 3,923 K, and the value of E_w is 7.84 kcal/mol. The activation energy of water permeation depicts the temperature-dependence of partial permeation flux, as it does in the case of ethanol. The effect of temperature on selectivity can therefore be predicted depending on the relative values of the activation energies of water and ethanol.

From the above description and the fact that the selectivity hardly depends on temperature, as seen in Fig. 5, the activation energy of ethanol could be expected to be the same as that of water. Regarding the order of magnitude in the activation energy and the little dependence of selectivity on temperature, it clearly appears that pervaporation can be greatly accelerated by operating at the highest temperature compatible with the heat-resistance of the membrane. When the effect of permeate pressure on the selectivity is neglected as shown in Fig. 5, the dependence of water flux on the temperature in the feed side and permeate pressure can be given according to the following equation:

$$J_w(T, P) = J_w(T^o, P^o) \cdot \exp\left[\left(\frac{E_w}{R}\right) \cdot \left(\frac{1}{T^o} - \frac{1}{T}\right)\right] \cdot \frac{RT \ln(x_w \gamma_w P_w^o / y_w P)}{RT \ln(x_w \gamma_w P_w^o / y_w P^o)} \quad (8)$$

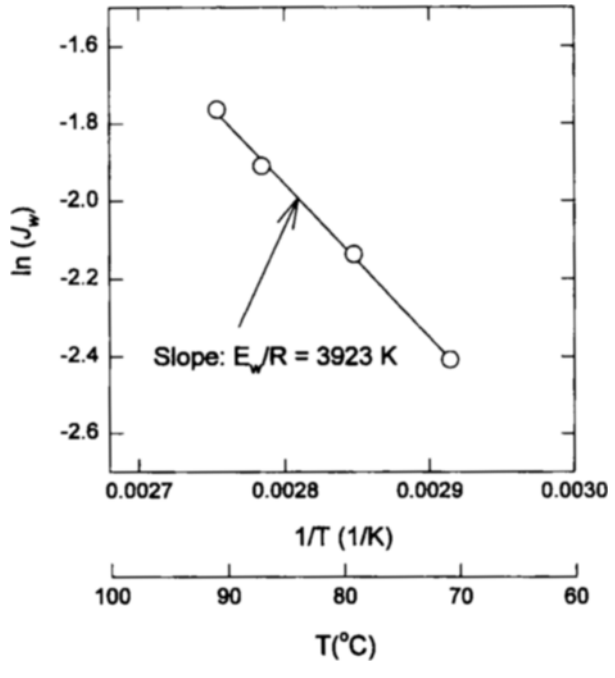

Fig. 8. Determination of Arrhenius coefficient in the Arrhenius plot of the water permeation flux through PVA membrane in the ethanol/water system.

where $J_w(T^o, P^o)$ is the water flux measured at a feed side temperature of T^o and permeate side pressure of P^o. Hence, $J_w(T^o, P^o)$ can only be a function of feed composition. The term on the influence of permeate pressure on water flux in Eq. (8) is derived from the fact that in the pervaporation the driving force for transport originates from the difference in chemical potential between feed and permeate [Mulder and Smolder, 1984]. The difference in chemical potential can be approximated as a difference in partial vapor pressures of the permeating component in the liquid feed and the gaseous permeate [Fleming and Slater, 1992; Wijmans and Baker, 1993].

Since the total flux is the sum of partial fluxes and the water content in the permeate is the ratio of water flux to total flux, the total flux, J_t, included in simulation equations can be expressed as the following equation.

$$J_t = J_w + J_e = \frac{J_w}{C_w^p} \quad (9)$$

To simulate a pervaporation system, one may observe from Eq. (8) and (9) that there should be membrane characteristic data such as $J_w(T^o, P^o)$, C_w^p and E_w/R together with thermodynamic data such as the activity coefficient and the saturated vapor pressure. The reference temperature and pressure were chosen as 78 °C and 11 mbar, respectively, in this study. At these operating conditions, the empirical equations for partial water permeation flux and permeate water composition are given by the following equations:

$$J_w = 3.935 \cdot C_w^f \quad (10)$$

$$C_w^p = \frac{12 \cdot C_w^f}{0.055 + 12.84 \cdot C_w^f - 7.7 \cdot C_w^{f2}} \quad (11)$$

The data on saturation vapor pressure required for calculating Eq. (8) were obtained by using the coefficients as tabulated by Daubert and Danner [1991], and the activity coefficient by using the coefficients for the van Laar equation as tabulated by Gmehling and Onken [1977]. The equations and coefficients are given in the following equations.

$$P_w^o = \exp(A + \frac{B}{T} + C \cdot \ln T + D \cdot T^E)$$
$$A = 7.3649 \times 10,\ B = -7.2582 \times 10^3,\ C = -7.3037$$
$$D = 4.1653 \times 10^{-6},\ E = 2 \quad (12)$$

$$\ln \gamma_w = A_{12} \cdot [A_{21}(1 - x_w)/\{A_{12}x_w + A_{21}(1 - x_w)\}]^2$$
$$A_{12} = 1.7769,\ A_{21} = 0.94 \quad (13)$$

where P_w^o and γ_w are the saturated vapor pressure and the activity coefficient of water, respectively, and x_w is the mole fraction of water in an ethanol/water mixture.

2. Comparison of Simulation and Continuous Mode Pilot Test Results

We considered two cases of continuous mode pilot tests: at a relatively low ethanol concentration range near the azeotropic point, and at a relatively high ethanol concentration range which is near pure ethanol. The operating conditions chosen are different from those in batch tests: higher feed side temperatures and lower permeate condensation temperatures. Therefore, the parameters had to be extrapolated, which could serve the reliability of simulation parameters. Based on

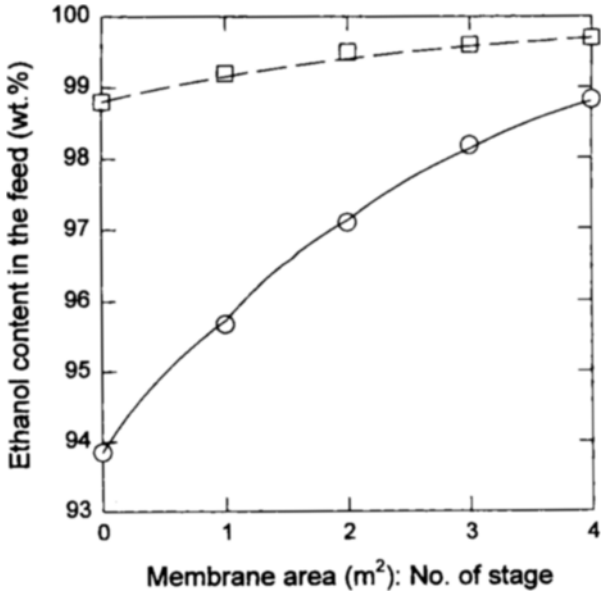

Fig. 9. Comparison of simulation and experimental data: Ethanol content in the feed for the membrane area with varying concentration range in the feed ethanol.
○, relatively low ethanol concentration; □, relatively high ethanol concentration; —, simulation at relatively low ethanol concentration; ---, simulation at relatively high ethanol concentration.

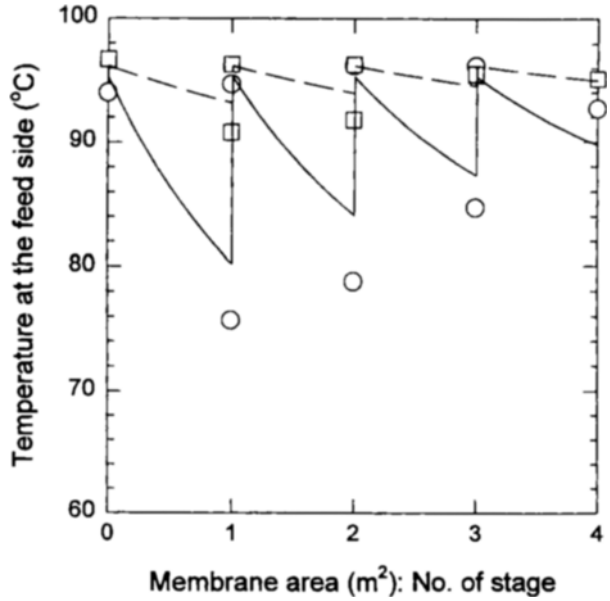

Fig. 10. Comparison of simulation and experimental data: Temperature at the feed side for the membrane area with varying concentration range in the feed ethanol.
○, relatively low ethanol concentration; □, relatively high ethanol concentration; —, simulation at relatively low ethanol concentration; --, simulation at relatively high ethanol concentration.

the empirical equations and data that were determined in the parameter estimation, we simulated the ethanol dehydration processes. The results are shown in Figs. 9 and 10, which give plots of feed concentration versus membrane area and the feed side temperature versus membrane area, respectively. It can be seen in Fig. 9 that the rate of increase in the feed ethanol content within the range of relatively low ethanol concentration is higher than in high ethanol concentration. This illustrates that the higher the feed water content, the higher the permeation fluxes. Fig. 9 shows that the simulation results give us good predictions of test results. The range in the feed flow rates during continuous mode pilot tests is lower than during batch mode pilot tests; nevertheless, the deviation of simulation from real test results is negligible, which means that there is no influence of flow rate on the flow pattern within the range from 15 to 80 *l*/h. As shown in Fig. 10, it is important to note that a temperature drop in the membrane module stage becomes very sensitive to the water content in the feed, resulting from the positive dependence of permeation flux on the water content in the feed. The heat of evaporation required for the permeating component is withdrawn from the liquid feed for the adiabatic pervaporation: a temperature drop can be observed between the liquid feed inlet and the liquid retentate outlet. However, in a practical pervaporation system, the process does not always progress under adiabatic conditions, which can describe the slight deviation between simulation and experimental results.

Combining the simulation results in Fig. 10 with those in Fig. 9 gives the typical pervaporation process under adiabatic conditions (See Fig. 11). Four linear functions of the partial permeation flux at temperatures of 80, 85, 90 and 95 °C

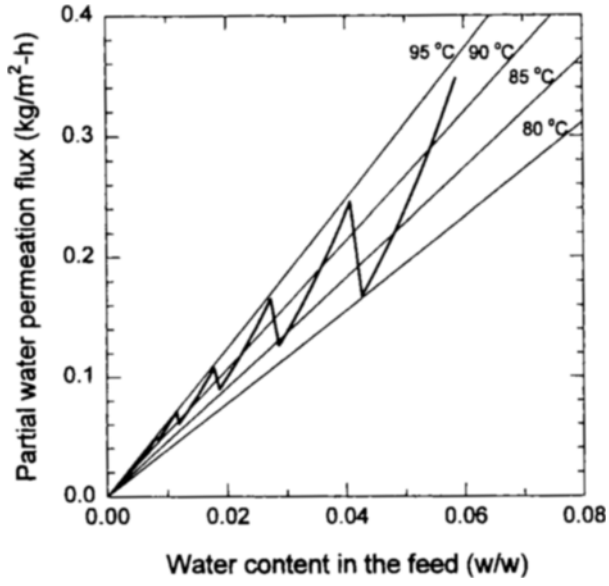

Fig. 11. Simulation results on the partial permeation flux of water for the water content in the feed: Pervaporation performance of multi-stage pervaporation membrane module with interstage reheater.

were determined by using Eq. (8) under isothermal conditions. As shown in Fig. 11, the partial permeation flux drops significantly with decreasing temperature of the feed side of the membrane. Therefore, in order to maintain high operating temperature, the pervaporation membrane module is generally subdivided into several stages between which interstage reheaters are installed. This can ultimately enhance the pervaporation

performance as a result of the reduction in membrane area required. Since the permeation flux is relatively high in the higher water feed concentration range, a high concentration gradient, together with a high temperature gradient, is obtained in the first stage of the membrane module.

CONCLUSION

A study of simulation on a pervaporation system for ethanol dehydration was done from a practical point of view. The simulation tool consisted of simulation equations, which describe mass and energy balances, and simulation parameters, which include the thermophysical properties of an ethanol-water mixture and the characteristic data of a PVA composite membrane for the separation of the ethanol-water mixture. Batch mode pilot tests enabled us to estimate the membrane characteristic data, which include the permeation flux and membrane selectivity and are empirically expressed as functions of feed composition and operating conditions such as feed side temperature and permeate pressure. We verified the suitability of simulation by a comparison of the simulation results and the real data obtained in a continuous mode pilot test, which indicates that the simulation predicts the continuous mode pilot tests within reasonable accuracy.

ACKNOWLEDGMENT

The authors are grateful to R&D Management Center for Energy and Resources (RaCER), Seoul, Korea for financial support.

NOMENCLATURE

A : membrane area [m^2]
C_w^f : water concentration in the feed side [w/w]
C_{wo}^f : water concentration in the feed side at the entrance of membrane module [w/w]
C_w^p : water concentration in the permeate side [w/w]
E_w : activation energy for water permeation [kcal/mol]
ΔH : latent heat of vaporization of permeate [kcal/kg]
ΔH_e : latent heat of vaporization of ethanol [kcal/kg]
ΔH_w : latent heat of vaporization of water [kcal/kg]
J_e : partial permeation flux of ethanol [kg/(m^2 h)]
J_t : total permeation flux [kg/(m^2 h)]
J_w : partial permeation flux of water [kg/(m^2 h)]
J_w^* : frequency factor in Eq. (7) [kg/(m^2 h)]
k : liquid heat capacity of feed [kcal/(kg K)]
k_e : liquid heat capacity of ethanol [kcal/(kg K)]
k_w : liquid heat capacity of water [kcal/(kg K)]
P^o : reference pressure on the permeate side in Eq. (8) [mbar]
P_w^o : saturated vapor pressure of water [mbar]
Q : feed flow rate [kg/h]
Q_o : feed flow rate at the entrance of membrane module [kg/h]
R : gas constant [kcal/(mol K)]
T : temperature on the feed side [K]
T_o : temperature on the feed side at the entrance of membrane module [K]
T^o : reference temperature on the feed side in Eq. (8) [K]
x_w : liquid mole fraction of water [mol/mol]
y_w : vapor mole fraction of water [mol/mol]

Greek Letter

γ_w : activity coefficient of water [-]

REFERENCES

Aptel, P., Challard, N., Cuny, J. and Neel, J., "Application of the Pervaporation Process to Separate Azeotropic Mixtures", *J. Memb. Sci.*, **1**, 271 (1976).

Binning, R. C., Lee, R. J., Jennings, J. F. and Martin, E. C., "Separation of Liquid Mixtures by Permeation", *Ind. Eng. Chem.*, **53**, 45 (1961).

Black, C., "Distillation Modeling of Ethanol Recovery and Dehydration Processes for Ethanol and Gasohol", *Chem. Eng. Progr.*, **September**, 78 (1980).

Chang, J.-H., Yoo, J.-K., Ahn, S.-H., Lee, K.-H. and Yoo, K.-O., "Development of Pervaporation System Simulator", *Membrane J. (Korean)*, **7**(1), 31 (1997).

Daubert, D. E. and Danner, R. P., "Physical and Thermodynamic Properties of Pure Chemicals: Data Compilation, Design Institute for Physical Property Data", AIChE., Hemisphere Publishing Corporation (1991).

Fleming, H. L., "Consider Membrane Pervaporation", *Chem. Eng. Progr.*, **July**, 46 (1992).

Fleming, H. L. and Slater, C. S., "Chapter 10. Pervaporation: Applications and Economics", Membrane Handbook, Ho, W. S. W. and Sirkar, K. K., eds., Van Nostrand Reinhold, New York (1992).

Gmehling, J. and Onken, U., "Vapor-liquid Equilibrium Data Collection, Aqueous-organic Systems", Dechema Chemistry Data Series, Vol. 1, Part 1, DECHEMA, Frankfurt am Main, Germany (1977).

Huang, R. Y. M. and Jarvis, N. R., "Separation of Liquid Mixtures by Using Polymer Membranes. II. Permeation of Aqueous Alcohol Solutions through Cellophane and Poly-(vinylalcohol)", *J. Appl. Polym. Sci.*, **14**, 2341 (1970).

Humphrey, J. L. and Seibert, A. F., "Separation Technologies: An Opportunity for Energy Savings", *Chem. Eng. Progr.*, **March**, 32 (1992).

Marin, M., Kalantzi, K. and Gilbert, H., "Pervaporation Process: Membrane Conditioning and Experimental Mass Transfer Analysis", *J. Memb. Sci.*, **74**, 105 (1992).

Mulder, M. H. V. and Smolder, C. A., "On the Mechanism of Separation of Ethanol/Water Mixtures by Pervaporation. I. Calculation of Concentration Profiles", *J. Memb. Sci.*, **17**, 289 (1984).

Mulder, M. H. V., Franken, A. C. M. and Smolder, C. A., "On the Mechanism of Separation of Ethanol/Water Mixtures by Pervaporation. II. Experimental Concentration Profiles", *J. Memb. Sci.*, **23**, 41 (1985).

Nguyen, T. Q., "The Influence of Operating Parameters on the Performance of Pervaporation Processes", *AIChE Symposium Series*, **82**(248), 1 (1986).

Rapin, J. L., "The Betheniville Pervaporation Unit-The First Large Scale Production Plant for the Dehydration of Ethanol", Proceedings of Third International Conference on Per-

vaporation Processes in the Chemical Industry, Englewood, NJ, 364 (1988).

Rautenbach, R. and Albrecht, R., "The Separation Potential of Pervaporation, part 1: Discussion of Transport Equations and Comparison with Reverse Osmosis", *J. Memb. Sci.*, **25**, 1 (1985a).

Rautenbach, R. and Albrecht, R., "The Separation Potential of Pervaporation, part 2: Process Design and Economics", *J. Memb. Sci.*, **25**, 25 (1985b).

Streicher, C., Kremer, P., Tomas, V., Hubner, A. and Ellinghorst, G., "Development of New Pervaporation Membranes, Systems and Processes to Separate Alcohols/Ethers/Hydrocarbons Mixtures", Proceedings of Seven International Conference on Pervaporation Processes in the Chemical Industry, Reno, Nevada, 297 (1995).

Tusel, G. F. and Bruschke, H. E. A., "Use of Pervaporation Systems in the Chemical Industry", *Desalination*, **53**, 327 (1985).

Wijmans, J. G. and Baker, R. W., "A Simple Predictive Treatment of the Permeation Process in Pervaporation", **79**, 101 (1993).

Yeom, C.-K., Dickson, J. M. and Brook, M. A., "A Characterization of PDMS Pervaporation Membranes for the Removal of Trace Organic from Water", *Korean J. Chem. Eng.*, **13**(5), 482 (1996).